

Melting of a quasi-one-dimensional Wigner crystal: Electrons on superfluid ^4He in a narrow channel

Hiroki Ikegami,* Hikota Akimoto, and Kimitoshi Kono

RIKEN, Hirosawa 2-1, Wako, Saitama, 351-0198, Japan

(Received 18 October 2010; published 17 November 2010)

We have investigated the melting process of electron crystals (or Wigner crystals) confined in quasi-one-dimensional channels 10–60 electrons in width, formed on the surface of superfluid ^4He , paying special attention to the nonlinear behavior in resistivity unique to the crystal phase, the Bragg-Cherenkov (BC) scattering of surface waves. We observed that the BC scattering disappears at a higher temperature for fewer electrons in the confined direction, indicating that the crystal-like structure persists to a higher temperature. We show that this behavior is understood in terms of a naive model describing how the positional correlation is disordered by free dislocations in the quasi-one-dimensional geometry.

DOI: [10.1103/PhysRevB.82.201104](https://doi.org/10.1103/PhysRevB.82.201104)

PACS number(s): 67.25.dj, 64.70.dj, 73.20.-r

The dimensionality of a system has a significant influence on the natures of phase transition and ordered states. It is generally accepted that in one-dimensional (1D) XY magnets, superfluids, and crystals, thermal fluctuations completely destroy the long-range order (LRO) at any finite temperature. In two-dimensional (2D) systems, the LRO is also destroyed but the weaker thermal effect allows the quasi-LRO to survive at low temperatures. The quasi-LRO is destroyed at a high temperature by the unbinding of pairs of topological defects, according to Kosterlitz and Thouless (KT).¹

In a quasi-1D geometry, such as in a strip or on the surface of a tube, the system shows 1D-like behavior when the coherence length is longer than the confining dimension whereas it is 2D-like in the opposite case. In such systems, fundamental questions arise as to whether the quasi-LRO develops at low temperatures and how the quasi-LRO is destroyed with increasing temperature. Experimentally, the superfluid has, surprisingly, been observed for ^4He films formed on the surface of long cylinders,^{2,3} which promoted many theoretical works.^{4–6} In the case of the melting of a crystal in the quasi-1D geometry, a number of computer simulations have been carried out for particles interacting with the Coulomb repulsion^{7,8} or other types of interactions,^{9,10} and most simulations suggest an interesting anisotropic melting process. However, there have been few experiments on the melting process in the quasi-1D geometry because a very clean system must be used to obtain a clear result.

In this Rapid Communication, we experimentally address the melting mechanism of electron crystals in a quasi-1D geometry by employing a very clean electron system, i.e., electrons formed on the superfluid ^4He .^{11,12} We carried out transport measurements of the electrons confined in micrometer-wide channels 10–60 electrons in width, paying special attention to the nonlinear transport unique to the electron crystal, the Bragg-Cherenkov (BC) scattering.^{13–16} The understanding of the properties of confined electrons on a micrometer scale is also of particular importance in the context of quantum information processing.^{17,18}

In a 2D system, the melting of a crystal is considered to be the KT-type transition but with a slight difference. A 2D

hexagonal crystal is characterized by the positional quasi-LRO and the sixfold-orientational LRO. According to the Kosterlitz-Thouless-Halperin-Nelson-Young (KTHNY) theory,^{19–21} these two orders are destroyed by two steps through an intermediate “hexatic” phase, which has no positional order while still possessing the orientational quasi-LRO. The melting of the crystal to the hexatic phase is driven by the dissociation of dislocation pairs and the transition from the hexatic phase to the fluid is caused by the unbinding of disclination pairs.

An electron crystal [or Wigner crystal (WC)] formed on liquid helium offers an excellent platform for studying 2D melting owing to its clean and flat surface without the pinning of dislocations. Although the hexatic phase has not been experimentally identified yet, experimental results, such as the universal jump in the shear modulus,^{22,23} support KTHNY melting. The melting takes place (presumably into the hexatic phase) at the plasma parameter $\Gamma \equiv U/K = 130 \pm 10$,^{11,12} where U and $K \equiv k_B T$ are the Coulomb potential and the kinetic energy per electron, respectively, (k_B is Boltzmann’s constant and T is temperature). In the WC phase, the localization of electrons causes the periodic deformation of the helium surface called the dimple lattice.^{11,12} Although the emergence of the dimple lattice has no influence on the melting temperature, the resultant coupling of electrons with the dimple lattice gives rise to the peculiar nonlinear transport arising from the BC scattering of surface waves (rippions).^{13–16} Because the presence of the dimple lattice is essential for BC scattering, the disappearance of BC scattering corresponds to melting in the 2D system.

We have investigated the melting process of the WC by transport measurements of electrons confined in channels 5, 8, and 15 μm in width W using devices such as the one shown in Fig. 1(a). The center channel forms a quasi-1D conduction path with length $L \sim 900 \mu\text{m}$, connecting two comb-shaped reservoirs of electrons. This long-channel geometry enables us to clearly observe nonlinear behaviors owing to the uniform driving electric field along the center channel.¹⁶ The device has a double-layered structure with top and bottom aluminum electrodes insulated by a SiO_2 layer [Fig. 1(c)]. The vertically etched channel is filled with capillary-condensed liquid ^4He . Its depth d is 1.7 μm for the

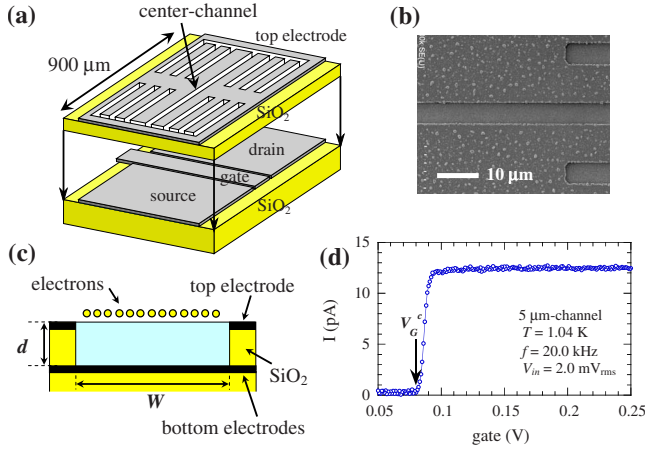


FIG. 1. (Color online) (a) Schematic of the device used for transport measurements. (b) Scanning electron microscopy image of the center channel of the 5 μm device. (c) Schematic vertical cross section of the channel. The device is located 0.5 mm above the level of bulk liquid ^4He and the channel is filled with capillary-condensed liquid. (d) Dependence of current on V_G for the 5 μm channel. The current is cutoff at V_G^c , giving an electron density of $5.82 \times 10^{12} \text{ m}^{-2}$.

5 and 8 μm channels and 1.4 μm for the 15 μm channel. Electrons charged on the liquid surface are confined in the channel by a negative voltage V_{top} applied to the top electrode. The bottom electrodes consist of a source, drain, and gate, which are positively biased with V_S , V_D , and V_G , respectively. Electrons in the reservoirs capacitively couple to the corresponding source or drain electrode located beneath the reservoirs. An ac voltage V_{in} (frequency $f = 20\text{--}100$ kHz) applied to the source induces current I_0 in the center channel and the induced current is detected by the drain. The electron velocity v is deduced from $v = I_0 / (enW)$. The resistance R of the center channel is obtained from the detected current by lumped-constant circuit analysis,¹⁶ and the mobility μ is deduced from $\mu = CL / (enWR)$, where $C \approx 1$ is a factor caused by the lumped-constant circuit analysis¹⁶ and is needed to reproduce the high-temperature theoretical mobility.²⁴ Data presented here were obtained at $V_{\text{top}} = -0.10$ V and $V_S = V_D = V_G = +0.25$ V. Electron density n is determined from the cutoff of the current [Fig. 1(d)] when V_G is negatively biased with respect to V_S using the relation $n = \epsilon\epsilon_0(V_S - V_G^c) / ed$,^{16,25} where V_G^c is the gate voltage at the cutoff. (e is elementary charge, ϵ_0 is vacuum permittivity, and ϵ is relative permittivity of liquid ^4He .) More experimental details are given in Refs. 16 and 26.

Figure 2 shows typical V_{in} dependences of the inverse of mobility μ^{-1} and electron velocity v at several fixed temperatures for the 5 μm channel. At low temperatures, μ^{-1} increases with increasing V_{in} , followed by a sharp drop. The increase in μ^{-1} is due to the drastic increase in the scattering rate arising from the BC scattering of ripplons, that is, the resonance of ripplons with the vertical oscillation of the surface caused by the moving dimple lattice. The BC scattering also gives rise to the saturation of the electron velocity at $v_1 = \omega(\mathbf{G}_1) / |\mathbf{G}_1|$,^{13,14,16} and it is clearly observed, as shown in Fig. 2(b), where $\omega(\mathbf{G}_1)$ is the ripplon angular frequency at

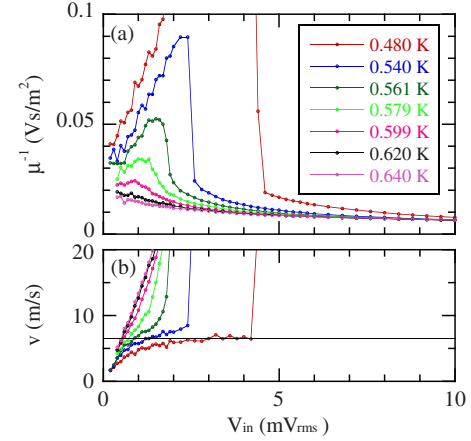


FIG. 2. (Color online) (a) μ^{-1} and (b) v as a function of V_{in} for the 5 μm channel at temperatures near $T_0 = 0.62 \pm 0.02$ K. The solid line in (b) represents $v_1 = \omega(\mathbf{G}_1) / |\mathbf{G}_1|$. Data were obtained at $f = 100.0$ kHz and $n = 5.64 \times 10^{12} \text{ m}^{-2}$.

the first reciprocal-lattice vector \mathbf{G}_1 of the WC. The drop in μ^{-1} at high V_{in} is attributed to the decoupling of the WC from the dimple lattice.¹⁶ The increase and the drop in μ^{-1} are smeared at high temperatures, and finally vanish. We define T_0 as the temperature at which the BC scattering disappears. In the case of the 2D system, the disappearance of the BC scattering corresponds to the melting transition, but in the quasi-1D geometry, it should be carefully interpreted, as discussed later.

The determination of T_0 from the dependence of μ^{-1} on V_{in} as in Fig. 2 was, however, time consuming, and so we employed this method only for the 5 μm channel. For the 8 and 15 μm channels, T_0 was determined from the temperature dependence of μ^{-1} measured at a small V_{in} (Fig. 3). The sharp rise in μ^{-1} at a certain temperature on cooling is caused by setting in the BC scattering, and this temperature is defined as T_0 . We confirmed that these two methods gave the same T_0 for the 8 μm channel at several electron densities. In contrast, for the 5 μm channel, the rounded tempera-

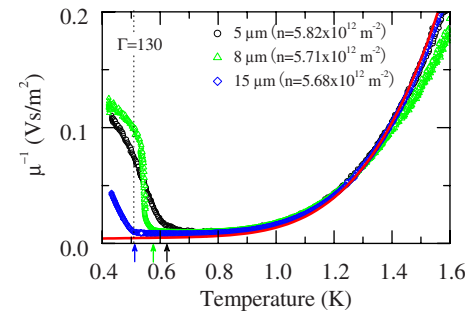


FIG. 3. (Color online) Temperature dependences of μ^{-1} for three channels at similar densities. The dotted line is the melting temperature for the 2D crystal ($\Gamma_m^{2D} = 130$). The arrows indicate T_0 determined from the temperature dependence (8 and 15 μm) or from the V_{in} dependence (5 μm). The solid line represents the theoretical result (Ref. 24) for a holding field of 5.0×10^4 V/m. Data were taken at $f = 20.0$ kHz and $V_{\text{in}} = 2.0$ mV_{rms} for 5 μm , $f = 100.0$ kHz and $V_{\text{in}} = 1.4$ mV_{rms} for 8 μm , and $f = 100.0$ kHz and $V_{\text{in}} = 2.0$ mV_{rms} for 15 μm channels.

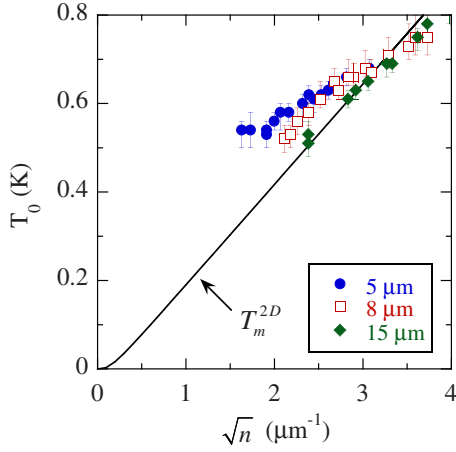


FIG. 4. (Color online) T_0 as a function of \sqrt{n} . The solid line is the melting temperature of the 2D crystal ($\Gamma_m^{2D}=130$) for the Coulomb interaction partially screened by the bottom electrodes located at $d=1.7 \mu\text{m}$.

ture dependence near T_0 (Fig. 3) prevented us from determining T_0 from the temperature dependence.

T_0 determined as above is summarized in Fig. 4 as a function of \sqrt{n} . In the figure, the melting temperature in the 2D system T_m^{2D} is also shown by the solid line. To evaluate T_m^{2D} , we use the partly screened Coulomb potential per electron $U=e^2/(4\pi\epsilon_0)(1/r_0-1/\sqrt{r_0^2+4d^2})$, because the average distance between electrons $r_0=(\pi n)^{-1/2}$ is comparable to d , and thus, the screening of the interaction by the bottom electrodes is not negligible (5–10 % depending on n). As seen in Fig. 4, T_0 for the 15 μm channel follows T_m^{2D} while T_0 for the 5 and 8 μm channels deviates to higher temperatures. The deviation is more significant for a narrower channel and at a lower density, that is, for a smaller number of electrons within the confined direction. This tendency is clearly seen in Fig. 5, where the plasma parameter Γ_0 at T_0 is plotted as a function of the number of electrons in the confined direction defined by $N\equiv\sqrt{n}W$; Γ_0 deviates from that in the 2D case ($\Gamma_m^{2D}=130$) and becomes smaller with decreasing N .

Now, we discuss the melting process of the WC in the quasi-1D geometry. The melting of the crystal is described

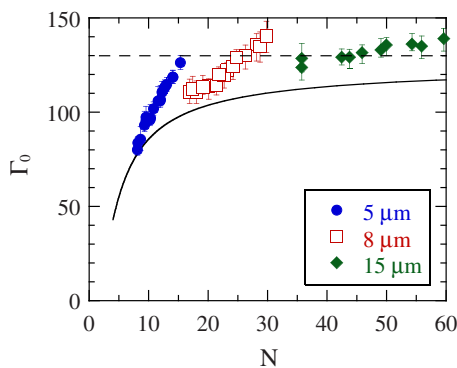


FIG. 5. (Color online) Γ_0 as a function of the number of electrons in the confined direction defined by $N=\sqrt{n}W$. The dashed line indicates the melting of the 2D WC ($\Gamma_m^{2D}=130$). The solid line represents $\xi_+=W$ (see text).

by the disordering process of the positional and orientational correlations. However, there have been no theoretical investigations of the disordering process of these two correlations in the quasi-1D geometry. Here, we consider only the positional correlation, and conduct a parallel discussion with the disordering process in a simpler and well-investigated system, the XY magnet in a quasi-1D geometry. In the quasi-1D XY magnet,^{4–6} thermally excited spin waves disturb the spin-spin correlation, making the correlation 1D-like at $r > w$ but 2D-like at $r < w$ at low temperatures; the correlation decays exponentially ($\sim e^{-r/\xi}$) at $r > w$ at low temperatures, whereas it shows power-law decay ($\sim r^{-\eta}$) at $r < w$,²⁷ where r is the distance between two positions, w is the dimension of the confined direction, and η and ξ are temperature-dependent constants. With increasing temperature, the $r^{-\eta}$ correlation at $r < w$ is destroyed because of the appearance of free vortices in the region $r < w$,^{4,5} leading to the crossover to the disordered state with the short-range correlation ($\sim e^{-r/\xi_+}$). The free vortices appear at a temperature at which the correlation length ξ_+ becomes comparable to w . ξ_+ is approximated as

$$\xi_+ \sim a \exp(b/t^\nu) \quad (1)$$

from KT theory, where $t \equiv T/T_{KT} - 1$ with the KT transition temperature T_{KT} , a is the diameter of a vortex core, and b is a nonuniversal constant related to the energy of the core. At the temperature characterized by $\xi_+ \sim w$, which is slightly higher than T_{KT} , the $r^{-\eta}$ -correlation changes to exponential decay ($\sim e^{-r/\xi_+}$).

We return to the WC in the quasi-1D geometry. At sufficiently low temperatures, the positional correlation is disturbed by thermal phonons, similarly to the quasi-1D XY magnet, giving rise to the positional correlation decaying as $r^{-\eta}$ at $r < W$ and $e^{-r/\xi}$ at $r > W$.¹⁰ Even though the positional correlation decays exponentially at large distances, our observation of the BC scattering indicates that the correlation length is sufficiently long below T_0 . In addition, our observation strongly indicates that the electrons within the correlation length maintain their relative positions for longer than the period of the vertical surface oscillation caused by the moving dimple lattice $\omega(\mathbf{G}_1)^{-1} \sim 10^{-8}$ s, otherwise the BC scattering should not occur.

The disappearance of the BC scattering is caused by the emergence of free dislocations for the reason described below. Following the same discussion as that for the XY magnet, free dislocations appear when the temperature is increased (i.e., the plasma parameter is decreased) and ξ_+ becomes comparable to W . The plasma parameter at which ξ_+ becomes equal to W is shown by the solid line in Fig. 5. The solid line is close to the experimentally obtained Γ_0 . To evaluate ξ_+ , we use $\nu=0.370$ from KTHNY theory^{20,21} and the relation $t=T/T_m^{2D}-1=\Gamma_m^{2D}/\Gamma-1$ with $\Gamma_m^{2D}=130$. We also assume the diameter of the core, which is on the order of the lattice constant, to be $a=n^{-1/2}$, and we take $b=1.8$, which corresponds to the core energy E_c estimated by the numerical calculation $E_c/k_B T_m^{2D}=4.9$.²⁸ (The relation between b and E_c is found in Ref. 29.) We should note that Eq. (1) is applicable only for $t < 7 \times 10^{-2}$ for $E_c/k_B T_m^{2D}=4.9$.²⁹ Although our

investigated range of t is out of this range, we expect the qualitative behavior to persist there. The similar behavior of the experimentally obtained Γ_0 to that of the solid line in Fig. 5 strongly indicates that the emergence of free dislocations causes the disappearance of the BC scattering. The free dislocations give rise to the rapid change in the relative positions of the electrons in a time shorter than $\omega(\mathbf{G}_1)^{-1}$, resulting in the disappearance of the BC scattering.

In conclusion, the melting of the WC in channels with 10–60 electrons in the confined direction was investigated through the nonlinear transport characteristic of the WC, that

is, the BC scattering. The plasma parameter at which the BC scattering disappears was found to decrease with a reduction in the number of electrons in the confined direction. This was explained by a naive model describing how the positional correlation of electrons is disordered by thermal phonons and free dislocations in the quasi-one-dimensional geometry, by recognizing the crucial role of free dislocations in the disappearance of the BC scattering.

This work is partly supported by PRESTO from JST, and a Grant-in-Aid for Scientific Research from MEXT, Japan.

*hikegami@riken.jp

- ¹J. M. Kosterlitz and D. J. Thouless, *J. Phys. C* **6**, 1181 (1973).
- ²K. Shirahama, M. Kubota, S. Ogawa, N. Wada, and T. Watanabe, *Phys. Rev. Lett.* **64**, 1541 (1990).
- ³H. Ikegami, Y. Yamato, T. Okuno, J. Taniguchi, N. Wada, S. Inagaki, and Y. Fukushima, *Phys. Rev. B* **76**, 144503 (2007).
- ⁴J. Machta and R. A. Guyer, *J. Low Temp. Phys.* **74**, 231 (1989).
- ⁵T. Minoguchi and Y. Nagaoka, *Prog. Theor. Phys.* **80**, 397 (1988).
- ⁶K. Yamashita and D. S. Hirashima, *Phys. Rev. B* **79**, 014501 (2009).
- ⁷G. Piacente, I. V. Schweigert, J. J. Betouras, and F. M. Peeters, *Phys. Rev. B* **69**, 045324 (2004).
- ⁸K. M. S. Bajaj and R. Mehrotra, *Physica B* **194-196**, 1235 (1994).
- ⁹R. Haghgooie and P. S. Doyle, *Phys. Rev. E* **70**, 061408 (2004).
- ¹⁰A. Ricci, P. Nielaba, S. Sengupta, and K. Binder, *Phys. Rev. E* **75**, 011405 (2007).
- ¹¹*Two-Dimensional Electron Systems on Helium and Other Cryogenic Substrates*, edited by E. Y. Andrei (Kluwer Academic, Dordrecht, 1997).
- ¹²Y. P. Monarkha and K. Kono, *Two-Dimensional Coulomb Liquids and Solids* (Springer-Verlag, Berlin, 2004).
- ¹³M. I. Dykman and Y. G. Rubo, *Phys. Rev. Lett.* **78**, 4813 (1997).
- ¹⁴W. F. Vinen, *J. Phys.: Condens. Matter* **11**, 9709 (1999).
- ¹⁵A. Kristensen, K. Djerfi, P. Fozooni, M. J. Lea, P. J. Richardson, A. Santrich-Badal, A. Blackburn, and R. W. van der Heijden, *Phys. Rev. Lett.* **77**, 1350 (1996).
- ¹⁶H. Ikegami, H. Akimoto, and K. Kono, *Phys. Rev. Lett.* **102**, 046807 (2009).
- ¹⁷P. M. Platzman and M. I. Dykman, *Science* **284**, 1967 (1999).
- ¹⁸D. I. Schuster, A. Fragner, M. I. Dykman, S. A. Lyon, and R. J. Schoelkopf, *Phys. Rev. Lett.* **105**, 040503 (2010).
- ¹⁹B. I. Halperin and D. R. Nelson, *Phys. Rev. Lett.* **41**, 121 (1978).
- ²⁰D. R. Nelson and B. I. Halperin, *Phys. Rev. B* **19**, 2457 (1979).
- ²¹A. P. Young, *Phys. Rev. B* **19**, 1855 (1979).
- ²²F. Gallet, G. Deville, A. Valdès, and F. I. B. Williams, *Phys. Rev. Lett.* **49**, 212 (1982).
- ²³G. Deville, A. Valdes, E. Y. Andrei, and F. I. B. Williams, *Phys. Rev. Lett.* **53**, 588 (1984).
- ²⁴M. Saitoh, *J. Phys. Soc. Jpn.* **42**, 201 (1977).
- ²⁵P. Glasson, V. Dotsenko, P. Fozooni, M. J. Lea, W. Bailey, G. Papageorgiou, S. E. Andresen, and A. Kristensen, *Phys. Rev. Lett.* **87**, 176802 (2001).
- ²⁶H. Ikegami, H. Akimoto, and K. Kono (unpublished).
- ²⁷P. Nightingale and H. Blote, *J. Phys. A: Math. Theor.* **16**, L657 (1983).
- ²⁸D. S. Fisher, B. I. Halperin, and R. Morf, *Phys. Rev. B* **20**, 4692 (1979).
- ²⁹A. J. Dahm, *Phys. Rev. B* **29**, 484 (1984).